Available online at www.sciencedirect.com
ScienceDirect
Polymer 48 (2007) 3809–3816
polymer
www.elsevier.com/locate/polymer

NMR determination of crystallinity for poly(ε-L-lysine)

Atsushi Asano*, Chikako Tanaka, Yoshifumi Murata

Department of Applied Chemistry, National Defense Academy, 1-10-20 Hashirimizu, Yokosuka, Kanagawa 239-8686, Japan

Received 6 February 2007; received in revised form 19 April 2007; accepted 19 April 2007
Available online 25 April 2007

Abstract

Crystallinity of poly(ε-L-lysine) (ε-PL) was discussed by analyzing the differences in the ^{1}H spin–spin relaxation times (T_2^H), the ^{13}C spin-lattice relaxation times (T_1^C), and the ^{13}C NMR signal shapes between the crystalline and the non-crystalline phases. The observed ^{1}H relaxation curve (free induction decay followed by solid-echo method) showed the sum of Gaussian and exponential decays. Similarly, the observed ^{13}C relaxation curves obtained from the Torchia method were double-exponential. The ^{13}C NMR spectrum of ε-PL was divided into the narrow and the broad lines by utilizing the intrinsic differences in the ^{1}H spin-lattice relaxation times in the rotating-frame between them, which are attributed to the crystalline and the non-crystalline phases, respectively. Even though the crystallinity is obtained from the identical NMR measurements, the estimated values are different with each other. The crystallinity estimated from the T_2^H differences was $75.8 \pm 0.1\%$ at 333 K and $60.7 \pm 0.4\%$ at 353 K. From the T_1^C differences, the value was estimated to be $62 \pm 11\%$. Furthermore, the value estimated from the NMR signal separation was $54 \pm 5\%$. In this study we have explained these discrepancies by the difference in susceptibility among the experiments for the inter-phase, which exists in-between the crystalline and the amorphous phases. Furthermore, the estimated crystallinity was ascertained by the X-ray diffraction experiment.

Keywords: Crystallinity; ^{13}C-T_1, ^{1}H-T_2, solid-state ^{13}C NMR; Poly(ε-L-lysine)

1. Introduction

Crystallinity is one of important physical and chemical properties for polymers. Actually, the crystalline phase structure or morphology may be more important and affect on the physical property of polymers; the same crystallinity but different morphology will cause a different physical or chemical property. However, the degree of crystallinity becomes an easy index, for example, for checking how the different polymerization process from the same raw materials affects the property of polymers, especially for industrial chemical purposes. Therefore, it is significant to know the accurate value of the crystallinity easily.

The crystallinity is defined as the volume or the weight fractions; we usually adopt the weight fraction as the crystallinity. There are a lot of methods to obtain the degree of crystallinity such as differential scanning calorimetry (DSC), X-ray diffraction, Raman and infrared (IR) spectroscopies, nuclear magnetic resonance (NMR), and so on [1,2]. However, it is well known that different methods provide the different crystallinity. This is ascribed to the difference in the susceptibility of an inter-phase among the observation methods, and also that the inter-phase is not clearly discriminated from both crystalline and amorphous phases by any observations: the determination of the border between the inter-phase and the crystalline or amorphous phases is not easy. Therefore, it is difficult to know the intrinsic degree of crystallinity.

Recently, it has been recognized that the observation of the solid-state ^{13}C NMR is very useful to determine the crystalline phase or the hard segment of polymers instead of the ^{1}H wide-line NMR, because the linewidth, the chemical shift value, and the ^{13}C spin-lattice relaxation time in the laboratory frame (T_1^C) of the solid-state ^{13}C NMR signal sensitively reflect the difference between the crystalline and the amorphous phases

* Corresponding author. Tel.: +81 46 841 3810; fax: +81 46 844 5901.
E-mail address: asanoa@nda.ac.jp (A. Asano).

0032-3861/$ - see front matter © 2007 Elsevier Ltd. All rights reserved.
doi:10.1016/j.polymer.2007.04.038

[3,4]. In general, ^{13}C NMR signal of a semi-crystalline polymer is consisted with narrow and broad components. The narrower signal is attributable to the crystalline phase, which polymer chains have higher order and lower mobility than that of the amorphous phase. The broader signal is ascribed to the non-crystalline phase mainly consisted with amorphous region, which polymer chains have lower order and higher mobility than that of the crystalline phase [3–5]. Furthermore, in many cases, the chemical shift values of both phases are different from each other because of the difference in both conformations: a solid-state ^{13}C NMR spectrum detects such a difference.

In the ^{1}H wideline NMR, we indirectly assume that the mobility of the crystalline phase is low, but that of the amorphous phase is high [2]. Nowadays, pulse ^{1}H NMR is often used to detect the crystallinity or hard segment of polymers by measuring the free induction decay (FID). The time constant of FID is governed by ^{1}H spin–spin relaxation time (T_2^H), which reflects the mobility straightforwardly. Therefore, the fraction of hard segment or the crystallinity can be estimated by fitting the FID with sum of several exponential, Gaussian, or Weibullian functions: the Weibullian function is explained by $\exp(-(t/T_2)^W)$, W is the Weible coefficient.

Similarly, the ^{13}C spin-lattice relaxation is useful to estimate the crystallinity, because the T_1^C value of the crystalline phase usually quite differs from that of the non-crystalline phase. The T_1^C value of the crystalline phase is, in general, much longer than that of the non-crystalline phase in solid polymers. Thus, the fraction of the long T_1^C component provides the degree of crystallinity.

However, since the T_1^C and T_2^H values are mainly governed by the mobility of polymer chains, the values largely depend on the observed temperature, and then the fraction is altered. Furthermore, if the inter-phase has the similar T_1^C value to that of the crystalline phase, we will be not able to distinguish the T_1^C value of the inter-phase from the T_1^C decay curve: here, we refer a thick interface layer which locates in-between the immobile crystalline and the mobile amorphous regions to an inter-phase. Especially, for the semi-crystalline polymers having the glass transition much higher than a room temperature, the molecular motion of inter-phase is very slow at a room temperature. Furthermore, in general, such a semi-crystalline polymer has a melting point much higher than 400 K, so that the molecular motions of crystalline and inter-phases will be similar with each other.

On the other hand, signal separation based on the intrinsic ^{1}H spin-lattice relaxation time in the rotating-frame ($T_{1\rho}^H$) into the narrow and the broad components also enables us to estimate the fraction of the crystalline phase [4,6]. These separated signals depend on the chain order not on the mobility. Therefore, it is possible very frequently that the crystallinity obtained from the ^{13}C relaxation curve and/or the ^{1}H FID signal analyses does not coincide with that estimated from the signal separation, even though the estimation is performed by the same solid-state ^{13}C NMR observations: this is because the origins of the obtained parameters are different between the relaxation and the spectral separation experiments. In general, the different methods give the different results for the degree of crystallinity as above mentioned. Therefore, one naively wants to estimate the identical value for the degree of crystallinity from NMR even though using the different parameters, such as signal separation and relaxation. However, for NMR observation, it is not exception that the different parameters provide the different crystallinity.

In this study, we clarify that the discrepancy is ascribed to the difference in sensitivity for detection of the inter-phase mobility, especially for a semi-crystalline polymer having a high crystallinity, a high glass transition temperature, and a high melting point. Semi-crystalline poly(ε-L-lysine) (ε-PL) is adequate to make a trial for detecting crystallinity, because ε-PL has high crystallinity, glass transition temperature, and melting point [7]. Furthermore, in order to ascertain the crystallinity obtained from NMR, we employed the X-ray diffraction (XRD) experiment and then compared the obtained values. Since XRD provides the crystallinity from the chain order not from mobility, the obtained value from XRD will be close to the value estimated from ^{13}C NMR signal separation.

2. Experimental

Poly(ε-L-lysine) (ε-PL: the unit structure is $-[NHCH_2CH_2CH_2CH_2CH(NH_2)CO]_n-$) is provided from Chisso Corporation, and the averaged degree of polymerization, n, is approximately 30. ε-PL is known as a semi-crystalline biodegradable hydrophilic polymer and nontoxic toward humans and environment [7]. ε-PL was first dissolved in methanol and its solvent cast sample was used for NMR experiments. The glass transition temperature and the melting point of ε-PL were measured by DSC with temperature increasing ratio of 2 K min^{-1}, and obtained at ca. 323 K and ca. 445 K, respectively.

For the X-ray diffraction (XRD) experiments, we prepared the mainly non-crystalline ε-PL sample. A ε-PL sealed in a glass tube with nitrogen atmosphere was heat-treated at 458 K for 20 min: the crystalline phase is completely melted. After the heat treatment, the glass tube is immediately immersed in liquid nitrogen to quench and keep the amorphous phase.

The solid-state ^{13}C NMR spectra are measured by the combined use of cross polarization (CP) and magic-angle spinning (MAS) with ^{1}H high-power dipolar-decoupling (CPMAS) techniques using Bruker DMX 500 spectrometer operating at 125.76 MHz for ^{13}C and 500.13 MHz for ^{1}H. The radio-frequency field strengths for both ^{13}C and ^{1}H were 55.6 kHz. The ^{1}H decoupling frequency was chosen to be 3 ppm down-field from tetramethylsilane (TMS) and the TPPM decoupling method [8] was used. The MAS frequency was set to 10 kHz and ^{13}C chemical shifts were measured relative to TMS using the methine carbon signal at 29.47 ppm for solid adamantane as an external standard. T_1^C decay was indirectly measured from protons through the CP enhancement as proposed by Torchia [9].

The ^{1}H spin–spin (transverse) relaxation time (T_2^H) was measured by the solid-echo method ($\pi/2-12\ \mu s-\pi/2-12\ \mu s$) using a JEOL MU25 pulse NMR spectrometer operating at 25 MHz for ^{1}H. We did not employ the 500 MHz instrument to detect ^{1}H signal, because of a problem of background of our probe for the high-resolution solid-state NMR. We never use a background suppression pulse sequence, because we worried about the signal loss, in particular, the signal come from the small amount of the inter-phase. The pulsed ^{1}H NMR is often used to detect the mobility of polymers.

XRD (X-ray diffraction) patterns were collected by using MAC Science M21X diffractometer with Cu Kα radiation of $\lambda = 0.154$ nm at 293 K.

3. Results and discussion

In order to detect a hard segment of polymers, ^{1}H NMR signals are frequently utilized, because the ^{1}H spin–spin (transverse) relaxation decay (T_2^H) for the hard segment is always faster than that of a soft segment, so that the signal attributed to the hard segment can be easily distinguished from the soft segment [10–12].

Fig. 1 shows the observed T_2^H decay curves at 0.585 T (^{1}H frequency is 25 MHz). These decays were obtained from the solid-echo pulse sequence at 353 K (a) and 333 K (b), respectively. These decays were very similar to that obtained from a single pulse method, except for the disappearance of the signal during the dead time of 10 μs after the pulse. Of course, the T_2^H is very convenient to investigate the amount of the crystalline phase or the hard segment. However, T_2^H values also depend on the difference in the mobility among the crystalline phase, inter-phase, and the amorphous phase, respectively, similar to the T_1^C measurement. The inter-phase, that we refer here, can be substituted for an immobile amorphous domain as named the rigid amorphous phase [13]. The inter-phase or rigid amorphous phase is actually close to the rigid and immobile crystalline phase, so that the mobility is more constrained than the amorphous phase as usual. The amorphous phase is, hereafter, attributed to a mobile phase rather than the inter-phase or the rigid amorphous phase.

The T_2^H decay observed at 353 K has apparently three relaxation times; one is Gaussian and the remains are exponential decays. We did not observe the Weibullian decay. On the contrary, the T_2^H decay at 333 K did not show such a decay curve consisting three components. The sum of one Gaussian and one exponential decays was appeared at 333 K. At room temperature, we could not observed the FID signals (not shown). Since both glass transition temperature and melting point of ε-PL are very high, the molecular motion of the inter-phase at 333 K is much less mobile and the T_2^H of the inter-phase becomes similar to that of the crystalline phase. Thus the fraction of Gaussian component consists of both inter-phase and crystalline phase, and becomes ca. 76%. This value will be over estimated.

The estimated fraction of the crystalline phase from Fig. 1(a) is $60.7 \pm 0.4\%$. The fractions of the inter-phase and the amorphous phase are, respectively, $20.8 \pm 0.1\%$ and $18.5 \pm 0.4\%$. It is hard to consider that the actual fraction of the inter-phase is mostly the same as that of the amorphous phase. Since the value of T_2^H depends on the mobility, the observation temperature influences the fractions of the inter-phase and the amorphous phase, in particular, the mobility of inter-phase will be obeyed by the immobile crystalline phase because of their close proximity with each other. At 353 K, the inter-phase is partially detected as a fraction of the crystalline phase. Similarly, the amorphous phase neighbored to the inter-phase is evaluated as the fraction of the inter-phase.

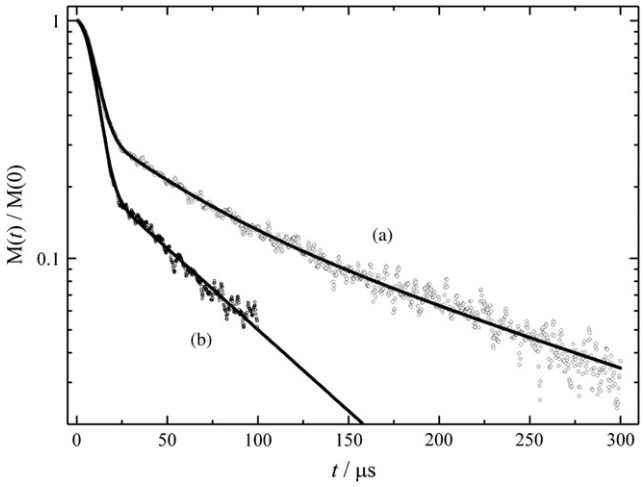

Fig. 1. Observed and normalized free induction decay by the solid-echo pulse sequence with the period of 12 μs between two π/2 pulses at 353 K (a) and 333 K (b). The horizontal line shows the echo time. The decay is least-square fitted by a Gaussian–exponential–exponential curve with the individual relaxation time as follows:

$$M(t)/M(0) = p_1 \times \exp\left(-0.5 \times (t/T_{2CR})^2\right) + p_2 \times \exp(-t/T_{2Int}) + (1 - p_1 - p_2) \times \exp(-t/T_{2Amor})$$

where the parameters of p_1 and p_2 represent the mole fractions of the crystalline phase and the inter-phase, respectively. For the decay shown in (b), the parameter p_2 is fixed to zero. The best-fit curves are depicted by a solid line and parameters are $p_1 = 0.607 \pm 0.004$, $p_2 = 0.208 \pm 0.010$, $T_{2CR} = 8.52 \pm 0.03$ μs, $T_{2Int} = 48 \pm 3$ μs, $T_{2Amor} = 177 \pm 8$ μs for (a). The values for (b) are $p_1 = 0.758 \pm 0.002$, $T_{2CR} = 8.29 \pm 0.02$ μs, $T_{2Amor} = 63.5 \pm 0.6$ μs. The symbols, CR, Int, and Amor in the above formula represent the crystalline phase, the inter-phase, and the amorphous phase, respectively.

Fig. 2 shows the observed ^{13}C CPMAS NMR spectrum of ε-PL obtained from methanol solvent cast method with the spin-locking periods of 1 μs (a) and 5 ms (b) prior to the CP contact time of 800 μs. The spectrum of Fig. 2(a) is absolutely the same as obtained from the conventional ^{13}C CPMAS NMR experiment, because the ^{1}H polarization does not mostly decay at such a short spin-locking time. Obviously, each signal contains both narrow and broad lines (see also Fig. 3). Recently, Maeda et al. have characterized the ε-PL by solid-state ^{13}C and ^{15}N CPMAS NMR, FT-IR, and Raman spectroscopy [14,15]. The present ^{13}C NMR spectrum in Fig. 2(a) resembles that of the observed one by them very much. The sharp and narrow signals are attributed to the crystalline phase, and the broad ones to the amorphous phase. Furthermore, the doublet

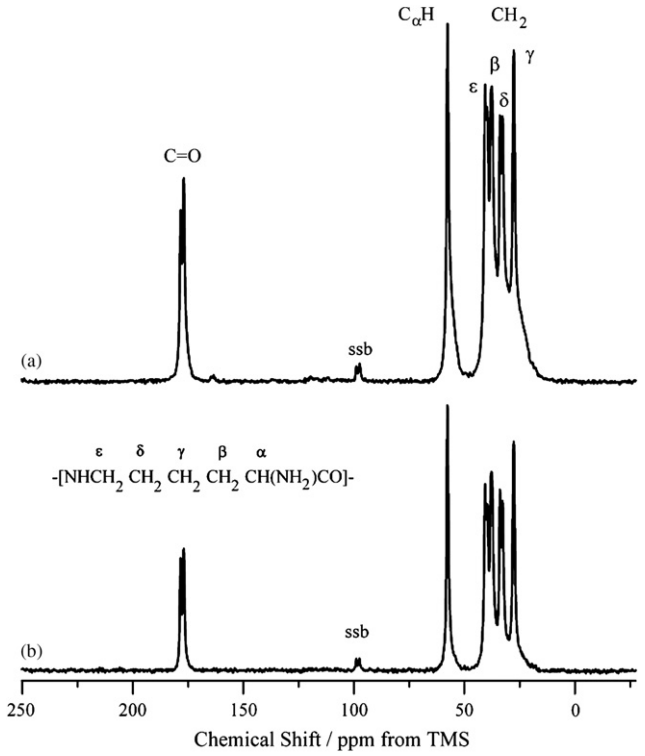

Fig. 2. Observed ^{13}C CPMAS NMR spectra of ε-PL with the spin-locking periods of 1 μs (a) and 5 ms (b). The peak assignments are also depicted in the figure. The symbol of ssb represents the artificial peak, spinning-side band at MAS of 10 kHz. The CP contact time of 800 μs is used.

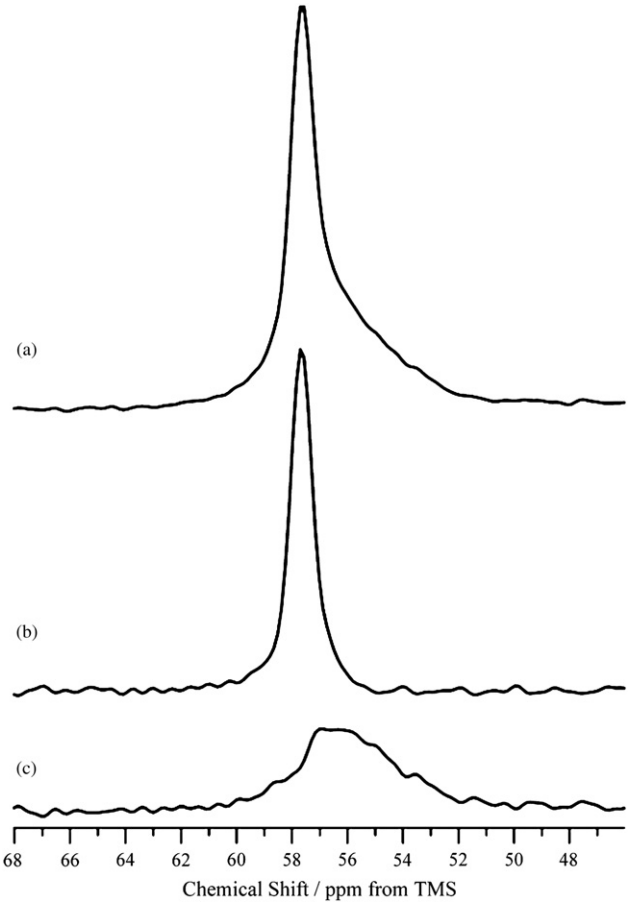

Fig. 3. Expanded ^{13}C CPMAS NMR spectrum at the $C_\alpha H$ region: (a) the same spectrum as that shown in Fig. 2(a); (b) the separated signal into the crystalline phase; and (c) into the non-crystalline phase.

peaks appeared at carbonyl (C═O), $CH_2(\varepsilon)$, and $CH_2(\delta)$ carbon signals perhaps indicate that the existence of two different crystalline phases [14].

Fig. 2(b), which is ^{13}C CPMAS NMR spectrum measured with the spin-locking time of 5 ms prior to the 800 μs CP contact time, shows that the intensity contribution from the narrow peaks is much greater than that in Fig. 2(a), and whole intensity also becomes weaker. The observed and apparent $T_{1\rho}^{H}$ values for the narrow peak of the $C_\alpha H$ carbon, which is attributed to the crystalline phase, was 24 ± 9 ms and for the broad peak 9.2 ± 0.9 ms. Hence, ^1H polarization decays much faster in the broad signals than in the narrow signals during the long spin-locking time of 5 ms. For a method of the signal separation into the crystalline or non-crystalline phases, it is necessary to make an intensity contrast between the crystalline and the non-crystalline phases as comparing to the spectrum in Fig. 2(a). The spin-locking time period of 5 ms was adequate to detect the intensities of both crystalline and non-crystalline phases.

The differences in the observed $T_{1\rho}^{H}$ value between the narrow and the broad signals are mostly due to the different molecular motion between them. However, the long $T_{1\rho}^{H}$ value is affected severely by the ^1H spin diffusion from the amorphous region; in solid, the ^1H spin-lattice relaxation is distorted by the ^1H spin diffusion phenomenon. Hence the relative ratio of the long $T_{1\rho}^{H}$ component does not provide the real and accurate contents of polymer chains with the slow molecular motion and then the degree of crystallinity. In contrast, T_1^C is little affected by the ^1H spin diffusion and monitors directly the difference in the molecular motion.

Fig. 4 shows the T_1^C decay curve of the $C_\alpha H$ carbon peak. The T_1^C decays were obtained by the Torchia pulse sequence [9]. The semi-log plot clearly indicates that the T_1^C decay is the double-exponential curve as same as that previously observed by Maeda et al. [14]. They estimated the crystallinity of ε-PL by analyzing the double-exponential T_1^C decay curves observed at each resonance to be 63%. The current T_1^C decay is also least-square fitted by the conventional double-exponential function and obtained that the fraction of the long T_1^C component is $62 \pm 11\%$. The obtained value is in excellent agreement with the previous one. The long component is assigned to the polymer chain with slow molecular motion for solid polymers. Polymer chains in the crystalline phase have much slower molecular motion than those in the amorphous phase. Therefore, the long component is ordinarily attributed to the crystalline phase.

For a semi-crystalline polymer, however, the inter-phase exists in-between the crystalline and the amorphous phases as shown in T_2^H experiment, so that the T_1^C decay will show a triple-exponential curve such as the T_1^C decay observed for polyethylene [3]. The observed T_1^C decay curve is not

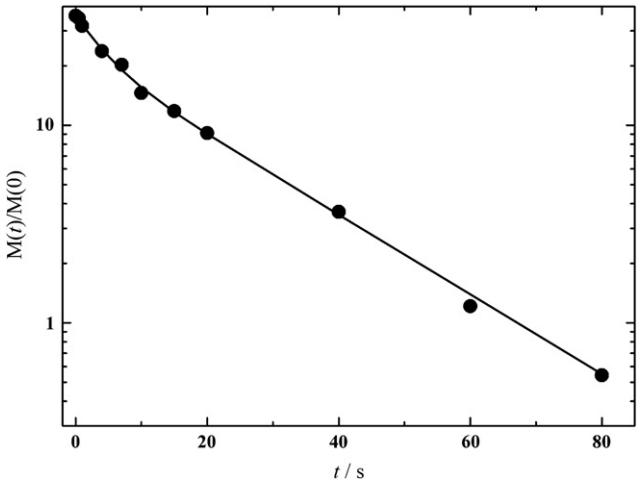

Fig. 4. The observed ^{13}C spin-lattice relaxation curve (●) obtained from the integral value of the $C_\alpha H$ signal. The solid line shows the results of the least-square fitting to the observed data points with a double-exponential function. The obtained T_1^C values are 4.4 ± 1.2 s and 22 ± 3 s for the short and long components, respectively. The relative ratio of the long component is 0.62 ± 0.11. The vertical is arbitrary unit.

a triple-exponential one. This implies that the molecular motion of the inter-phase will be similar to either crystalline or amorphous phases, and then that the obtained crystallinity from the T_1^C measurement is over estimated. In order to confirm this, we applied the signal separation method into the crystalline and the non-crystalline (inter-phase and amorphous) phases [4,6].

Fig. 3(a) shows the expanded ^{13}C CPMAS NMR spectra of Fig. 2(a) for the $C_\alpha H$ carbon region. The signal consists of both narrow and broad peaks. The narrow peak is attributed to the crystalline phase and the broad one to the non-crystalline phase; non-crystalline phase includes both amorphous and inter-phase regions. We separated the spectrum into both narrow and broad signals by employing the differences in the intrinsic $T_{1\rho}^H$ value that characterize the crystalline and the amorphous regions [4,6].

Fig. 3(b) and (c) are linear combinations of the spectra of Fig. 2(a) and (b) obtained from the different spin-locking times where we have attempted to null the non-crystalline and crystalline signal contributions, respectively. Spectrum of Fig. 3(a) is completely reproduced by sum of spectra of Fig. 3(b) and (c). It is noteworthy that both separated spectra of Fig. 3(b) and (c) depend on the difference in chain order only but not in molecular motion.

The chemical shift of the broad peak illustrated in Fig. 3(c) moves toward the upper magnetic field (the lower frequency) as compared to that of the narrow one in Fig. 3(b) by 1.4 ppm. This is due to the difference in the conformation between the crystalline and the non-crystalline phases. According to the γ-*gauche* effect on the ^{13}C chemical shifts, this slight upper-field shift for the broad signal of the non-crystalline phase is reasonable because the conformation of ε-PL in the non-crystalline phase is predicted to be *gauche*-rich as polyethylene [1] and that in the crystalline phase is expected to be *trans*-zigzag rich like a γ-form of nylon 6 [14].

The integrals of both spectra in Fig. 3(b) and (c) provide the relative contribution of the crystalline phase. Of course, the CP experiment distorts the intensity between the crystalline and non-crystalline phases during CP contact time. We examined the CP dependency with various CP contact times from 25 μs to 7 ms, to obtain the relative CP efficiencies for both crystalline and non-crystalline phases at CP contact time of 800 μs. The obtained values for the crystalline and the non-crystalline phases are 0.789 and 0.969, respectively. By using these efficiencies, we estimated the relative contribution of the crystalline phase to be 0.54. Since standard uncertainty of this estimation is 0.03–0.05 [4,6], the obtained crystallinity of ε-PL from the spectral separation based on the differences in the intrinsic $T_{1\rho}^H$ values becomes $54 \pm 5\%$.

This value is not in accord with that obtained from the T_1^C analysis. The estimated crystallinity from the T_1^C analysis is larger than that from the signal separation by approximately 10%. This discrepancy comes from the dealing with the inter-phase, which exists in-between the crystalline and amorphous phases. In the signal separation, the broad signal shown in Fig. 3(c) includes the inter-phase, because the conformation of the inter-phase is not ordered higher than that of the crystalline phase. This implies that the crystallinity estimated from the separation of ^{13}C CPMAS NMR spectrum into the crystalline and non-crystalline components reflects the real crystallinity rather than the T_1^C experiment.

Each T_1^C decay curve for the narrow and the broad signals is also obtainable. If the broad signal in Fig. 3(c) comes from both the amorphous and the inter-phase regions, the T_1^C decay will show a non-single exponential curve. Similarly the T_1^C decay of the crystalline phase, that is narrow component, shows a single-exponential. We divided each ^{13}C spectrum observed by the Torchia pulse sequence [9] into the narrow and the broad components by comparing with the line shapes of Fig. 3(b) and (c) or by a deconvolution using a few Gaussian functions [16], and obtained each signal intensity.

It is clear that the T_1^C decay curve of the crystalline phase (narrow component) is single-exponential (Fig. 5(a)) and that of the non-crystalline phase (broad component) is non-single exponential (Fig. 5(b)). Sum of both decays equal to the curve shown in Fig. 4. For the crystalline component, we obtained the T_1^C value of 25 ± 2 s by least-square fit to the conventional single-exponential curve. This value is in good agreement with the value of the long T_1^C component that estimated by a double-exponential curve illustrated in Fig. 4. This observation indicates that the narrow signal contains the ordered polymer chains in the crystalline phase only.

On the other hand, for the non-crystalline component, the observed data points are difficult to be lease-square fit to a double-exponential function as well as a single-exponential function, because of multi-exponential curvature. Fig. 5(b) shows that the non-crystalline phase consists of several components with various molecular motions, which affects the ^{13}C spin-lattice relaxation. The broken and dotted-broken lines in Fig. 5(b) represent, respectively, the short and long T_1^C decay components obtained from the T_1^C decay curve shown in Fig. 4. If the broad component is consisted of polymer chains

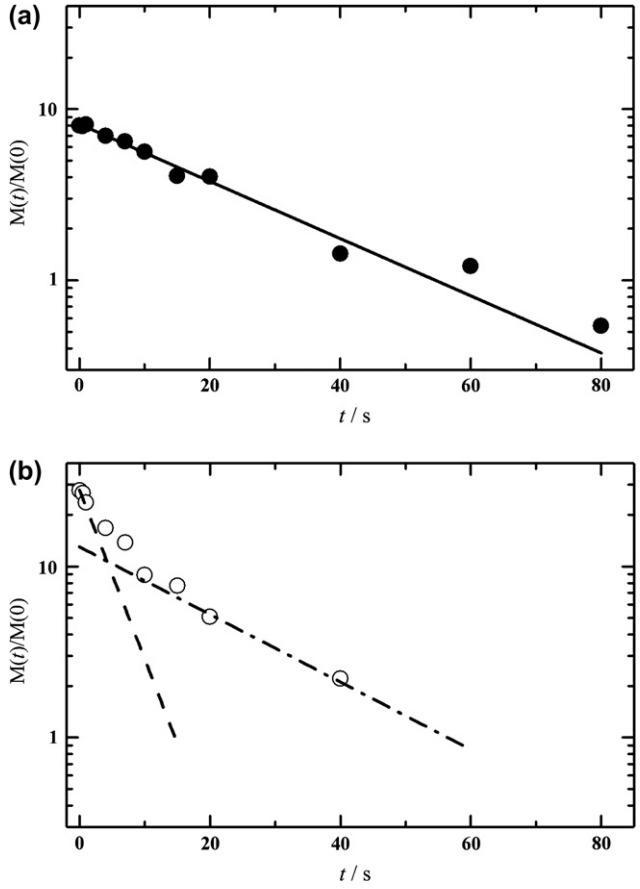

Fig. 5. The observed ^{13}C spin-lattice relaxation curves obtained from the integrals of (a) the crystalline signal of Fig. 3(b) and (b) the non-crystalline signal of Fig. 3(c). The solid line in (a) is least-square fit to the obtained integral data points with a single-exponential decay. The broken and dotted-broken lines in (b) show the short and long T_1^C components estimated in Fig. 4, respectively. The vertical is arbitrary unit.

in the amorphous phase only, the T_1^C decay will show a single-exponential curve with T_1^C value of 4–5 ms. Fig. 5(b) clearly proves that the broad component includes both inter-phase and amorphous regions.

Meanwhile, it is also important to discuss the reasonability and accuracy of the value of crystallinity determined from NMR. We employed the X-ray diffraction (XRD) experiment to estimate the crystallinity for the same ε-PL sample that is used for NMR measurements. Although the crystallinity obtained from XRD may not fully correspond to that from NMR as we mentioned above, XRD pattern reflects the chain order not mobility so that the estimated value will be comparable to that obtained from signal separation method.

It is necessary to know the characteristic XRD pattern of the amorphous phase to estimate the crystallinity from the XRD. In order to detect the XRD pattern of the amorphous phase, we measured mostly the non-crystalline ε-PL sample, which is made by rapid quench of heated ε-PL beyond its melting point. When we measured the solid-state ^{13}C NMR spectrum of the quenched ε-PL, it shows weak intensity of a typical narrow peak attributed to the crystalline phase on the large amount of the broad signal as shown in Fig. 6. Interestingly, the XRD pattern of the quenched ε-PL shows little diffraction ascribed the crystalline phase. This indicates that the XRD reflects only the large amount of crystalline domain but the NMR can detect clearly the tiny amount of them even though the phase forms very small domain and microcrystalline structure. Actually, the XRD pattern also shows a very small peak of the microcrystalline phase at ca. $2\theta = 19^\circ$. Therefore, this sample is not completely amorphous but may exist microcrystalline phase. It has been discussed that the ^{13}C solid-state NMR spectrum can be easily affected by the microcrystalline phase and shows higher resolution and enhancement [17].

Fig. 7 shows the XRD patterns of normal (a) and quenched (b) ε-PL samples and its linear combination (c). The crystallinity can be estimated by both integrals of the XRD patterns of (a) and (c). Since the XRD patterns of (a) and (b) are obtained from the different samples, the absolute intensity is different from each other. In Fig. 7, the XRD pattern of (b) is attenuated by a factor. Therefore, the estimated crystallinity has uncertainly of 5–10% depending on the factor. The estimated value is about 58%. This value is comparable to that obtained from the ^{13}C NMR signal separation experiments within an experimental error. Furthermore, the value of 58% is in-between of the estimated from T_2^H at 353 K (60.7%) and ^{13}C NMR signal separation (54%). This estimated value is, however, thought to be close to the upper limit because it is necessary to be larger value of crystallinity that the XRD pattern of (b) shown in Fig. 7 should be much weaker. Namely, much smaller factor is required and it is necessary to be more intense for the XRD pattern (c). The envelope of the pattern (a), which is consisted of mainly non-crystalline phase, seems to be more intense. Thus, the crystallinity estimated from the subtraction of XRD patterns is possible to be much lower value than 58%.

Furthermore, we observed the ^{13}C DDMAS (dipolar-decoupling MAS) NMR spectrum of ε-PL to estimate the crystallinity. The ^{13}C DDMAS NMR spectrum provides the intrinsic intensity for both crystalline and non-crystalline phases, while the ^{13}C CPMAS spectrum is distorted by their CP efficiencies. However, we cannot divide the ^{13}C DDMAS NMR spectrum into the contributions from crystalline and non-crystalline regions through the ^{13}C DDMAS experiment like a ^{13}C CPMAS experiment. Therefore, we used the NMR spectrum of crystalline phase obtained from ^{13}C CPMAS experiment shown in Fig. 3(b) to estimate the contribution from non-crystalline phase through the ^{13}C DDMAS NMR spectrum. The calculated crystallinity from the area integrals of the whole ^{13}C DDMAS NMR spectrum and its non-crystalline phase contribution was 53%. This value is in excellent agreement with that estimated from ^{13}C CPMAS NMR experiment. This fact proves that the estimation from the CP experiment with the correction of the CP efficiency provides the accurate crystallinity even though the CP distorts the signal intensities.

Consequently, we conclude that the ^{13}C NMR spectral separation provides crystallinity corresponding to the chain order as XRD experiments easily and accuracy rather than T_1^C and T_2^H experiments, which depend on molecular motion.

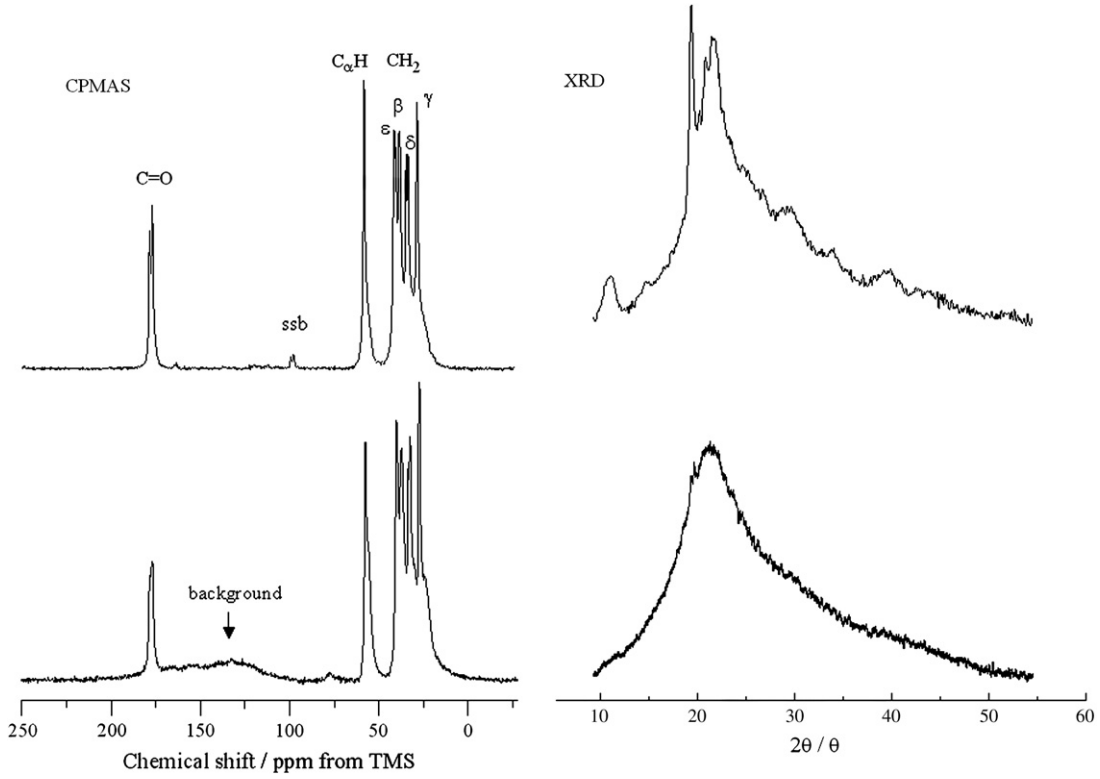

Fig. 6. Comparison between the ^{13}C CPMAS NMR spectra and the XRD patterns obtained from the pristine ε-PL cast from methanol (above figures) and ε-PL mainly consisted of non-crystalline phase (bottom figures). The ^{13}C CPMAS NMR spectrum of the pristine ε-PL cast from methanol is the same as that shown in Fig. 2(a). It is clear that the ^{13}C CPMAS NMR shows the existence of crystalline phase as sharp peaks but the XRD pattern does not suggest the existence.

We summarized and illustrated the possible morphology detected by T_2^H, T_1^C, and ^{13}C NMR signal separation experiments in Fig. 8.

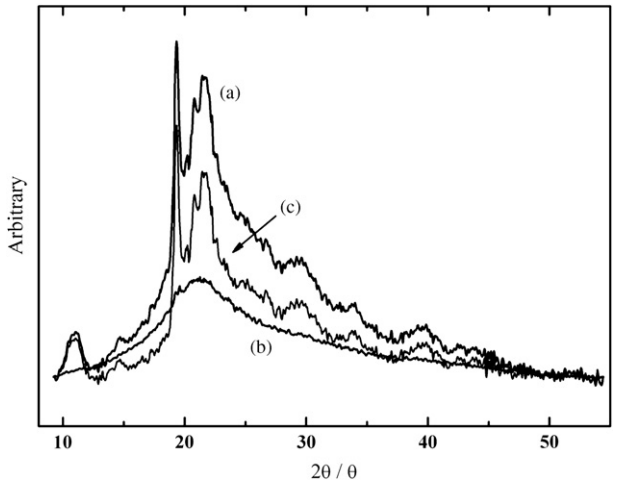

Fig. 7. Observed X-ray diffraction patterns of (a) pristine ε-PL cast from methanol, (b) ε-PL mainly consisted of non-crystalline phase, and (c) difference pattern obtained by subtraction of attenuated (b) from (a). The difference pattern (c) can be altered by the choice of the attenuated parameter, *f*, because the intrinsic absolute intensity is different between (a) and (b). Here, we selected the *f* value that the intensity at $2\theta =$ ca. 13° becomes to be zero. In this case, the crystallinity can be estimated to be approximately 58% by using the integrals of XRD patterns of (a) and (c).

4. Conclusion

The above observations suggest that the crystallinity detected by the T_1^C measurement is over estimated, and the intrinsic value is close to 54% for ε-PL. Fig. 8 shows the schematic illustration of the typical lamellar structure with the susceptive difference among the present three detections. The crystallinity estimated from the relaxation is largely affected by the molecular motion and similarly by observation temperature. On the other hand, the signal separation produces only the spectrum ascribed from the crystalline phase, because the chain order as well as the molecular motion influences the ^{13}C NMR spectrum. However, the signal separation method is not valid to detect the inter-phase, because the ^{13}C NMR signals of both the inter-phase and the amorphous phase appear as a broad line.

In conclusion, when the molecular motion of the inter-phase is similar to that of the crystalline phase, namely the T_1^C value is very close to that of the crystalline phase, the inter-phase region is not detectable from the T_1^C measurement. Especially, in the case of semi-crystalline polymers with high crystallinity such as ε-PL, the molecular motion of the inter-phase is strongly restricted by the stable and much amount of the crystalline phase. Similarly, when the molecular motion of the inter-phase is close to that of the amorphous region, the component is not also detectable correctly by the T_1^C measurement and the obtained crystallinity will be less estimated.

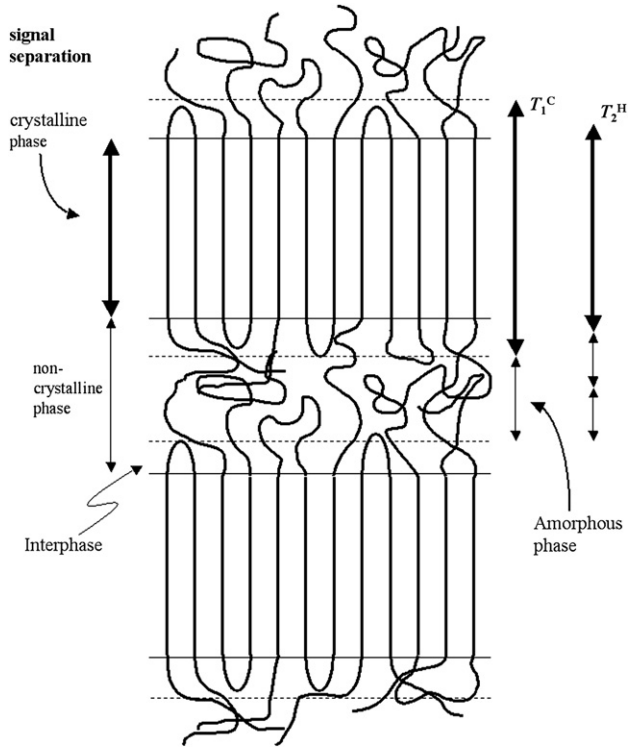

Fig. 8. Schematic illustration of the typical lamellar structure of a semi-crystalline polymer. The arrows indicate the differences in susceptibility among the signal separation, T_1^C and T_2^H measurements, respectively. These arrows are expected for the ε-PL that has the high crystallinity. For detecting the crystallinity from T_2^H measurement, these three phases are probably correctly distinguished if the measuring temperature is chosen to obtain those individually. However, we cannot know which temperature classify them correctly and individually.

Therefore, to estimate the crystallinity of semi-crystalline polymers, it is necessary to employ both methods of the signal separation and the T_1^C experiment. In particular, it is better to execute the signal separation experiment when the observed T_1^C decay does not show a triple-exponential curve.

Acknowledgement

We are grateful to Prof. Kurotsu, who kindly allows us to use his pulsed NMR instrument, JEOL MU25, without any qualifications.

References

[1] Strobl GR. The physics of polymers. Berlin Heidelberg: Springer-Verlag; 1996 [chapter 4].
[2] Kitamaru R, Kaji K. Kobunshi Jikken-gaku. In: Kobunshi no Kotai Kouzou II (Solid structure of polymers II), vol. 17. Tokyo: Kyoritsu Shuppan Co., Ltd; 1984 [chapter 6].
[3] Yamanobe T. In: Ando I, Asakura T, editors. Solid state NMR of polymers. Amsterdam: Elsevier; 1998 [chapter 7].
[4] VanderHart DL, Asano A, Gilman JW. Chem Mater 2001;13:3781–95.
[5] When the measured temperature is much higher than T_g, the mobile amorphous phase can be observed as a sharp and narrow signal due to the reduction of $^1H-^1H$ dipolar interaction by rapid molecular motion like a liquid.
[6] VanderHart DL, Pérez E. Macromolecules 1986;19:1902–9.
[7] Shih IL, Shen MH, Van YT. Bioresour Technol 2006;97:1148–59.
[8] Bennet AE, Rienstra CM, Auger M, Lakshmi KV, Griffin RG. J Chem Phys 1996;103:6951–8.
[9] Torchia DA. J Magn Reson 1978;30:613–6.
[10] Gerstein BC. In: Komoriski RA, editor. High resolution NMR spectroscopy of synthetic polymers in bulk. Florida: VCH Publishers; 1986 [chapter 9].
[11] Tanaka H, Nishi T. J Appl Phys 1986;59:1488–92.
[12] Ikehara T, Nishi T. Polymer 2000;41:7855–64.
[13] Wunderlich B. Prog Polym Sci 2003;28:383–450.
[14] Maeda S, Kunimoto K, Sasaki C, Kuwae A, Hanai K. J Mol Struct 2003;655:149–55.
[15] Maeda S, Mori T, Sasaki C, Kunimoto K, Kuwae A, Hanai K. Polym Bull 2005;53:259–67.
[16] For every spectrum obtained from the Torchia pulse sequence, the signal separation into the crystalline and the non-crystalline phases is done by comparing with Fig. 3(b) or (c). We also employed the deconvolution technique by a sum of Gaussian functions to detect the integrals at the every delay period in the Torchia pulse sequence. Two Gaussian functions are used to reproduce the antisymmetric line shape of Fig. 3(c). Obtained decays from both methods, that is signal separation and deconvolution, showed a good coincidence with each other.
[17] Wickramasinghe NP, Kotecha M, Samoson A, Past J, Ishii Y. J Magn Reson 2007;184:350–6.